JOURNAL OF COMPUTATIONAL PHYSICS **131,** 48–53 (1997)
ARTICLE NO. CP965416

# The Mass-Damped Riemann Problem and the Aerodynamic Surface Force Calculation for an Accelerating Body

Zhiqiang Tan,† Dennis Wilson,§ and Philip L. Varghese†

†*Department of Aerospace Engineering and Engineering Mechanics and* §*Institute for Advanced Technology, University of Texas at Austin, Austin, Texas 78712*

Received August 1, 1994; revised September 28, 1995

We consider an extension of the ordinary Riemann problem and present an efficient approximate solution that can be used to improve the calculations of aerodynamic forces on an accelerating body. The method is demonstrated with one-dimensional examples where the Euler equations and the body motion are solved in the non-inertial co-ordinate frame fixed to the accelerating body. © 1997 Academic Press

## 1. INTRODUCTION

The objective of this note is to provide an improved method for computing the trajectory of an object that moves due to fluid pressure forces. In CFD calculations, the most important final results are probably the aerodynamic forces. Conventionally, the body forces and moments are obtained by integrating the *flow pressure* on the solid boundary [1]. That is, the same pressure from the flow calculation is used to predict the body motion. We shall label this approach the *conventional method*. This approach looks obvious and natural, and it would seem that the accuracy in force calculation can be improved only after improving the flow calculations. However, it will be shown that improved force calculations can be obtained without improving the accuracy of the flow computation and, indeed, the conventional method may give erroneous results if the body acceleration is very large.

THE MASS-DAMPED RIEMANN PROBLEM. This problem may be described as follows: The left half of a long tube is initially filled with an ideal gas with state $w_L = (\rho_L, u_L, p_L)^T$ and the right half is filled with gas with state $w_R = (\rho_R, u_R, p_R)^T$. Here $\rho$ is the gas density, $u$ is the velocity, and $p$ is the pressure. At $x = 0$, there is a piston with mass $m$ and cross sectional area $A$. The piston moves freely in the tube, and friction between the piston and the walls, viscous forces, and gravity are neglected. The speed history of the piston is to be calculated.

Because the piston size does not influence the solution, we assume it to be infinitesimally thin. The $x$-$t$ graph of the mass-damped Riemann problem in the lab coordinate system is shown in Fig. 1. The standard Riemann problem is a special case of the mass-damped problem and corresponds to $m = 0$. The $x$-$t$ graph is shown in Fig. 2. In the standard Riemann problem, $\rho_L^* \neq \rho_R^*$, but $u_L^* = u_R^* \equiv u^*$ and $p_L^* = p_R^*$. In the mass-damped Riemann problem, $\rho_L^* \neq \rho_R^*, u_L^* = u_R^* \equiv V$, the piston velocity, and $p_L^* \neq p_R^*$. The pressure difference is required to accelerate the piston.

Let us consider the piston motion at an early stage (from $t = 0$ to $t = \Delta t$) only. From Fig. 1, the force acting on the piston is proportional to the star pressure difference: $F^* = A(p_L^* - p_R^*)$. When the conventional method is used, the flow pressures $p_L$ and $p_R$ are used instead of $p_L^*, p_R^*$ to calculate the surface forces, $F = A(p_L - p_R)$. When $m/A$ is large, it will be shown that $F$ is very close to $F^*$ and no problem arises. However, when $m/A \to 0$, an explicit integration of Newton's equation $V^1 = V^0 + \Delta t\, F/m$ would give infinite velocity, while we know that $V$ is always bounded from the property of the Riemann problem (see Fig. 1). Because $F$ is a function of the left and right states in the conventional approach, and thus a constant, no implicit mechanism is provided and therefore explicit integration has to be performed. On the other hand, when the star pressures are used, implicit integration is possible because the star pressures are functions of $u^*$ and, hence, $V$. With implicit time integration, $V$ can be bounded.

This example not only shows the difficulty of the conventional method but also indicates the solution; i.e., we should use the star pressures instead of the flow pressures to calculate the force on the moving body.

In solving 1D problems numerically, the following strategy can be applied. Suppose the flow field and piston position and speed are known at $t^{(n)}$; we first solve the mass-damped Riemann problem during time $t^{(n)}$ and $t^{(n+1)}$, to get the relationship between $p^*$ and $u^*$. Then we solve the Newton equation $du^*/dt = A/m\,[p_L^*(u^*) - p_R^*(u^*)]$ implicitly, to get $u^*$ $(=V)$ at $t^{(n+1)}$.



0021-9991/97 $25.00

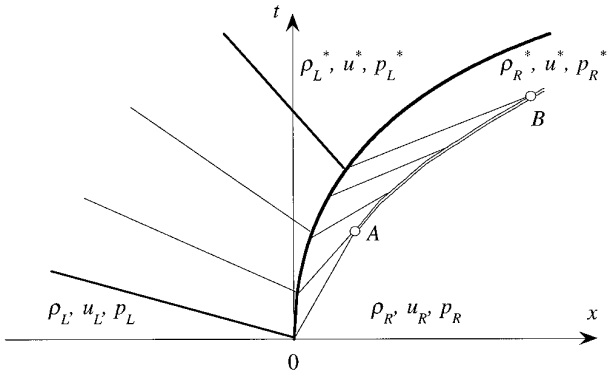


**FIG. 1.** The $x$-$t$ graph of the mass-damped Riemann problem. The star pressures $p_L^*$ and $p_R^*$ are different.

In this note, we shall perform a preliminary analysis on the behavior of the mass-damped Riemann problem and propose an efficient approximate solution. Then we shall briefly describe how to apply the idea of using star pressures to general problems and how to incorporate an Euler equation solver with the body motion solver. Finally, we shall demonstrate the advantages of the new force calculation method by two examples.

## 2. THE MASS-DAMPED RIEMANN PROBLEM AND THE BODY MOTION CALCULATION

*Formulation in 1D*

We assume the gas is inviscid and perfect. Extension to nonperfect gases is possible but is beyond the scope of this note. In the standard Riemann problem, the solution, which is a function of $x/t$, can be found analytically. In the mass-damped problem, such a similarity solution no longer exists. To understand the difficulty in solving the problem, just note that one side is always compressed. It is known that a shock-compression wave interaction problem is difficult, if not impossible, to solve analytically (cf. [2]). Therefore, an approximate formulation of the mass-damped Riemann problem is considered.

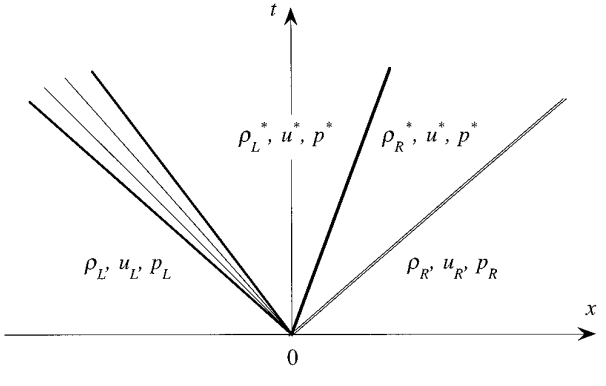


**FIG. 2.** The $x$-$t$ graph of the standard Riemann problem.

Consider the right side of the piston (Fig. 1). The basic assumption of the approximation is that the star region is connected with the right state through a single wave rather than, say, a combination of a compression wave and a shock wave. In the general case, this single wave can be either a simple wave or a shock wave. For either wave, the relation [2, 3]

$$\psi(p_R^*/p_R) = -\frac{u_R - u^*}{a_R}\sqrt{\gamma}, \tag{1}$$

holds, where $\gamma$ is the specific heat ratio, $a$ is the speed of sound, and $\psi$ is a function defined by

$$\psi(s) \equiv \begin{cases} \dfrac{s-1}{\sqrt{\gamma_+ s + \gamma_-}}, & s \geq 1, \\ \dfrac{\sqrt{\gamma}}{\gamma_-}[s^{\gamma_-/\gamma} - 1], & s < 1, \end{cases} \tag{2}$$

with $\gamma_\pm \equiv (\gamma \pm 1)/2$. The case $s \geq 1$ corresponds to the Rankine–Hugoniot relation for shock waves and $s < 1$ corresponds to simple waves. For details, see [2 or 3].

Similarly, the left state can be linked with the left star region through a single wave and the following relation holds:

$$\psi\left(\frac{p_L^*}{p_L}\right) = +\frac{u_L - u^*}{a_L}\sqrt{\gamma}. \tag{3}$$

The single wave approximation is exact when there is no simple wave–shock wave interaction. This is true in the early stages or late stages of the solution. Note that in numerical time-stepping, the time step size is usually small for accuracy. Therefore, the approximate star pressures $p_L^*$ and $p_R^*$ used in the numerical solution should be accurate.

The inversion of $\psi(s)$ can be found to be

$$s(\psi) \equiv \begin{cases} 1 + \dfrac{\psi^2}{2}\left[\gamma_+ + \left(\gamma_+^2 + \dfrac{4\gamma}{\psi^2}\right)^{1/2}\right], & \psi \geq 0, \\ \left[\max\left(0, 1 + \dfrac{\gamma_-}{\sqrt{\gamma}}\psi\right)\right]^{\gamma/\gamma_-}, & \psi < 0, \end{cases} \tag{4}$$

where the maximum function is added to include the vacuum situation. Note that $s''(\psi)$ is continuous at $\psi = 0$ and $s'(\psi) \geq 0$ for all $\psi$. Therefore, the piston motion equation has the following explicit form:

$$\dot{u}^* = \frac{A}{m}\left[p_L\, s\left(\sqrt{\gamma}\,\frac{u_L - u^*}{a_L}\right) - p_R\, s\left(\sqrt{\gamma}\,\frac{u^* - u_R}{a_R}\right)\right] \equiv f(u^*). \tag{5}$$

When the flow states $(p_L, u_L, a_L)$ and $(p_R, u_R, a_R)$ are known on the piston surface, Eq. (5) can be solved implicitly.

Qualitative Behavior of the Mass-Damped Riemann Problem. Let the equilibrium solution of Eq. (5) (i.e., the solution of $f(u^*) = 0$) be $u_0$. It is, of course, also the solution of the standard Riemann problem. We expand $f(u^*)$ at this point to get $f(u^*) = (u^* - u_0)\, f'(\xi)$, where $\xi$ is a point between $u_0$ and $u^*$ and $f'(u^*) \equiv df/du^*$. Here we have used the fact that $f(u_0) = 0$ and that $s'$ (hence $f'$) is continuous. If we treat $f'(\xi)$ as a known function of $t$, the solution of Eq. (5) is

$$u^* = u_0\,(1 - e^{g't}) < u_0 \quad \text{for } t > 0$$

because $g' < 0$, where $g'$ is the average of $f'(\xi)$ in $(0, t)$. We also have

$$\frac{d(u^{*2})}{dt} = 2\,u_0^2\, g'\,(1 - e^{g't}) < 0 \quad \text{for } t > 0.$$

Therefore, the piston is monotonically accelerated from $u^*(0) = 0$ to $u^*(\infty) = u_0$. The process is quite smooth in that no oscillation occurs. Although this conclusion is based on a single wave approximation, we expect it also to hold for the exact solution.

Numerical Method for Eq. (5). Even with the single wave approximation, an exact solution of the resulting equation (Eq. (5)) is not available in general. Note that an iterative solution is necessary even for the standard Riemann problem. Therefore, a numerical solution must be sought. Here the first-order implicit time-stepping is illustrated. Extension to higher-order schemes is straightforward. The discrete equation is

$$[1 - \Delta t\, f'(u^{*(n)})]\,(u^{*(n+1)} - u^{*(n)}) = \Delta t\, f(u^{*(n)}). \tag{6}$$

In the special case $u^{*(n)} = u_L = u_R$, Eq. (6) reduces to

$$\frac{u^{*(n+1)} - u^{*(n)}}{\Delta t} = \frac{(A/m)[p_L - p_R]}{1 - \Delta t\, f'(u^{*(n)})}.$$

On the other hand, the conventional method yields

$$\frac{u^{*(n+1)} - u^{*(n)}}{\Delta t} = \frac{A}{m}\,[p_L - p_R].$$

Thus, it is seen that the only difference is that the magnitude of the force in the new method has been reduced by a factor $1/[1 - \Delta t\, f'(u^{*(n)})]$. If $\Delta t\, f'(u^{*(n)}) \to 0$, due to a small time step or a large mass, the new method is equivalent to the conventional method.

*Remark.* The iterations (6) can be viewed as a switched evolution–relaxation scheme for the equilibrium solution. In particular, when $\Delta t\, A/m \to \infty$, we have a new Newton iterating scheme for the standard Riemann problem.

## 3. STAR PRESSURE CALCULATION FOR GENERAL FLOW PROBLEMS

The idea of the damped Riemann problem can be extended to general flow problems and to higher dimensions. We assume that the star region near a point $\mathbf{r}$ on the body is small, so the piston analogy applies locally. Equations (1) and (3) now become

$$\psi\left(\frac{p^*(\mathbf{r})}{p(\mathbf{r})}\right) = \mathbf{n} \cdot \frac{\mathbf{v}(\mathbf{r}) - \mathbf{u}^*(\mathbf{r})}{a(\mathbf{r})}\sqrt{\gamma}, \tag{7}$$

where $p$ is the flow pressure, $\mathbf{u}^*(\mathbf{r})$ is the local body velocity, $\mathbf{v}$ is the flow velocity, and $\mathbf{n}$ is the *inward* normal of the body (i.e., the outward normal of the fluid region).

Newton's second law has the form

$$m\,\dot{\mathbf{V}} = \int_{\Gamma_w} p^*(\mathbf{r})\,\mathbf{n}\, d\Gamma_w, \tag{8}$$

where $\Gamma_w$ is the body boundary and $\mathbf{V}$ is the translational velocity. In addition to translation, body rotation must also be included. The angular momentum equation gives

$$\mathrm{I} : \dot{\omega}^* = \int_{\Gamma_w} p^*(\mathbf{r})\,\mathbf{r} \times \mathbf{n}\, d\Gamma_w \tag{9}$$

in 3D, where $\omega$ is the angular velocity vector, I is the moment of inertia tensor of the body, and the origin is chosen to be at the center of mass. Since $\mathbf{u}^*(\mathbf{r}) = \mathbf{V} + \omega \times \mathbf{r}$, elimination of $p^*(\mathbf{r})$ from Eqs. (8) and (9) using Eq. (7) gives a closed differential system for $\mathbf{V}$ and $\omega$ when the flow solutions $p(\mathbf{r})$, $\mathbf{v}(\mathbf{r})$ and $a(\mathbf{r})$ are known. This system can be solved implicitly in the same manner as Eq. (6).

## 4. COUPLING WITH FLOW SOLVERS

The Euler equations for 1D compressible, inviscid flow of a perfect gas are

$$w_t + f_x + s = 0, \tag{10}$$

where

$$w = \begin{bmatrix} \rho \\ \rho u \\ e \end{bmatrix}, \quad f = \begin{bmatrix} \rho u \\ \rho u^2 + p \\ u(e+p) \end{bmatrix},$$

and $e$ is the total energy. Other terms have been defined previously.

The source term is defined as

$$s = \rho \begin{bmatrix} 0 \\ \dot{V} \\ \dot{V}u \end{bmatrix}. \tag{11}$$

Note that $\dot{V}$ represents the acceleration of a flow particle due to the noninertial motion of the reference frame. In order to use existing codes with fixed grids, the equations are written in a computational coordinate system fixed on the body.

The source term is treated via time-splitting to avoid changing existing Euler codes. We first write

$$\frac{w' - w^{(n)}}{\Delta t} + \rho^{(n)} \begin{pmatrix} 0 \\ \dot{V} \\ \dot{V}u - \frac{1}{2}\Delta t\, \dot{V}^2 \end{pmatrix}^{(n)} = 0; \tag{12}$$

then the Euler equations are advanced by $\Delta t$ without the source term by writing

$$\frac{w^{(n+1)} - w'}{\Delta t} + f_x = 0, \tag{13}$$

where $w'$ is the intermediate state from the Euler step. Note that the energy equation correction term is different from $\dot{V}u$ in Eq. (11). The extra term $\Delta t\ \dot{V}^2/2$ in Eq. (12) was obtained by requiring the pressure to be unchanged after the source correction stage. Since both the density and pressure are unchanged in the source correction step, no negative values appear in the square root calculation for the sound speed, provided the density and pressure given by the Euler solver are all nonnegative. Therefore, in this respect the robustness of the code is the same as the Euler solver. In the present procedure the source term is added first. An alternative is to advance the Euler equations first and then to correct the source term in the second half-step.

The above time-stepping procedure is first-order accurate. Other standard schemes such as second-order time stepping, second-order splitting procedure, and implicit methods could also be applied.

## 5. EXAMPLE CALCULATIONS

In this section, two 1D examples are given to show the improvement in accuracy obtained by using the new force calculation method. Further applications can be found in [4], where we computed the motion of a projectile in an axisymmetric blast wave accelerator. The sourceless Euler equations (Eqs. (10)) are solved on uniform grids. Roe's approximate Riemann solver [5] with the MUSCL approach is used. A description of the Euler procedure can be found in [6]. In the following, $\gamma = 1.4$ is assumed.

Expansion Problem. Here the left side of the piston is initially filled with gas at state $(\rho_L, u_L, p_L)^{\mathrm{T}} = (10^2\ \mathrm{kg/m^3}, 0\ \mathrm{m/s}, 10^7\ \mathrm{Pa})^{\mathrm{T}}$ and the right side is the vacuum which is approximated by $(\rho_R, u_R, p_R)^{\mathrm{T}} = (10^{-5}\ \mathrm{kg/m^3}, 0\ \mathrm{m/s}, 10^{-5}\ \mathrm{Pa})^{\mathrm{T}}$. The mass/area ratio of the piston is $m/A = 40\ \mathrm{kg/m^2}$.

Only expansion waves exist on the left. Therefore $\psi < 0$, and Eq. (5) reduces to a single differential equation given by

$$\dot{u}^* = \frac{A}{m} p_L \left[1 - \frac{\gamma_-}{a_L} u^*\right]^{\gamma/\gamma_-} \tag{14}$$

with the initial condition $u^*(0) = 0$. Here we have used the fact that $u_L = 0$. The exact solution of Eq. (14) is

$$u^* = \frac{a_L}{\gamma_-}\left[1 - \left(\frac{\gamma_+ p_L A}{m a_L} t + 1\right)^{-\gamma_-/\gamma_+}\right]$$

which is well known within the internal ballistics community [7].

The numerical results were obtained on a uniform grid. Two mesh sizes $\Delta x = \frac{1}{8}$ m and $\frac{1}{32}$ m were used with constant CFL number 0.5. The piston travel $X$, piston speed $V$, and force $\Delta p^*$ with $\Delta x = \frac{1}{32}$ m computed by the new method are compared in Fig. 3 with the analytical solution. Excellent agreement is found for all curves, except that the surface force at early times is not very smooth. This should not be surprising, considering the severe change in pressure at this stage.

The results of the conventional method and the new method are compared in Fig. 4. This figure compares the errors in piston speed obtained by the two methods for two different mesh sizes. It can be seen that the error produced by the new method is much lower than the error by the conventional method.

Piston Accelerated by a $M_s$-10 Shock. In this problem, the right half space and a left portion between $x =$

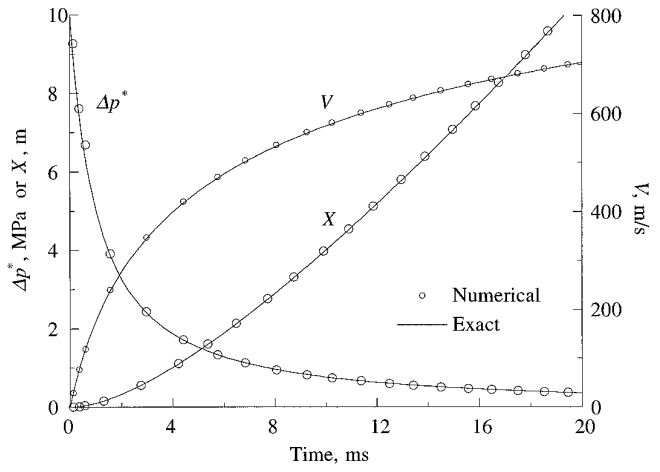


**FIG. 3.** The expansion problem. Piston travel, speed, and force variation in the lab coordinate system.

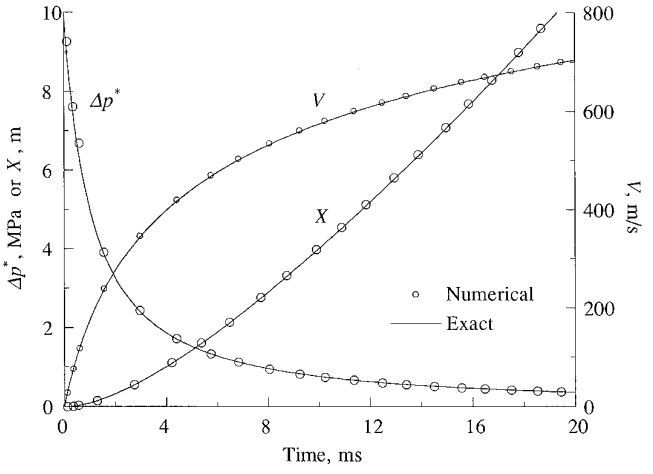


**FIG. 5.** The shock–piston interaction problem. Travel, speed, and force variation in the lab coordinate system. $m/A = 50\ \mathrm{kg/m^2}$. Comparison of the numerical solution with the single wave approximate analytical solution.

$-3$ m and $x = 0$ is initially at $\rho = 1\ \mathrm{kg/m^3}$, $u = 0$, and $p = 10^5$ Pa. A $M_s = 10$ shock is placed at $x = -3$ m and moving toward the piston, so the initial state in $x < -3$ m is $\rho = 5.714\ \mathrm{kg/m^3}$, $u = 3087$ m/s, $p = 116.5 \times 10^5$ Pa.

Although this is not a mass-damped Riemann problem, an approximate analytic solution is still possible, if we assume that after the shock hits the piston wall, the gas state behind the reflected shock does not change during the whole process. This assumption is valid as long as the expansion behind the shock is slow or weak. Thus, we can again apply the single wave approximation after the shock hits the wall, in that the left star region is connected to the constant state of the reflected shock through a simple (expansion) wave. From a straightforward shock calculation the time when the shock hits the wall is found to be $t = 0.8018$ ms, and the reflected shock state is $\rho = 19.58\ \mathrm{kg/m^3}$, $u = 0$ m/s, and $p = 885.4 \times 10^5$ Pa. This state is used as the left state of the mass damped Riemann prob-

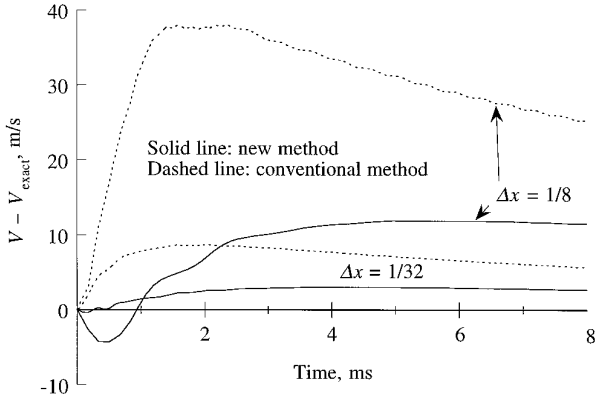


**FIG. 4.** Travel and speed errors of the new force method and the conventional method.

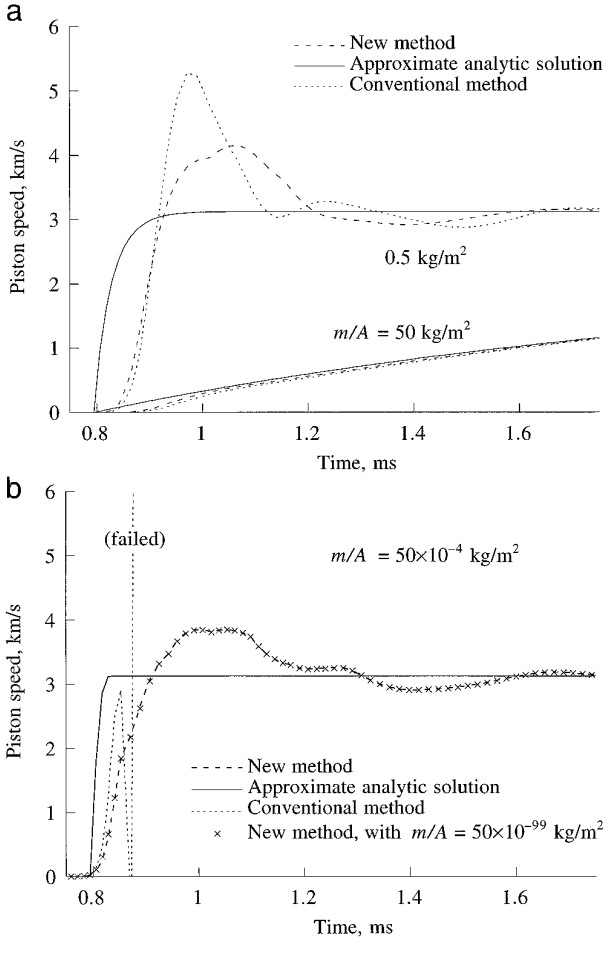


**FIG. 6.** Comparison of the new method, conventional method, and the approximate analytical solution for force calculation, for the shock-piston interaction problem at various mass-area ratios. (a) $m/A = 50\ \mathrm{kg/m^2}$ and $50 \times 10^{-2}\ \mathrm{kg/m^2}$. (b) $m/A = 50 \times 10^{-4}\ \mathrm{kg/m^2}$ and $50 \times 10^{-99}\ \mathrm{kg/m^2}$.

lem. Then Eq. (5) can be easily integrated numerically to give the piston trajectory at any time after 0.8018 ms.

The numerical results were obtained with a CFL number of 0.5 and $\Delta x = \frac{1}{8}$ m. A uniform grid was again used. The piston trajectory and surface force are shown in Fig. 5 for $m/A = 50$ kg/m$^2$. The agreement between the numerical method and the analytical approximate solution is quite good. Still better agreement was achieved with a smaller mesh size $\Delta x = \frac{1}{32}$ m (not shown here).

More calculations were performed using smaller $m/A$ for both the conventional method and the new method. The calculated piston velocities are shown in Figs. 6a and 6b. It can be seen that when $m/A$ is reduced, both the new and conventional solutions suffer from oscillations. However, the oscillations of the conventional method were more severe when $m/A$ became smaller and finally blew up when $m/A = 50 \times 10^{-4}$ kg/m$^2$. On the other hand, the present method was quite stable for all $m/A$ values we tested from $m/A = 50 \times 10^{-4}$ to $50 \times 10^{-99}$ kg/m$^2$. Indeed, using the present method the oscillations are almost the same magnitude at $m/A = 50 \times 10^{-99}$ kg/m$^2$ as at $50 \times 10^{-4}$ kg/m$^2$.

At large times, there is a small difference in piston speeds calculated by the numerical method and the approximate analytical solution. This is observed consistently at all $m/A$ values. The discrepancy is mainly due to the inaccuracy of the single wave approximation at large times. In fact, the equilibrium piston velocity should be the same as the incoming shock speed 3087 m/s. Our numerical results oscillate slowly about this value within narrow bounds. The oscillations are probably due to the long wavelength errors of Roe's method for slowly moving shocks [8], rather than the force calculation method or the source correction method. (The shock simulated here *is* slowly moving in the computational coordinate system.) On the other hand, the equilibrium state of the approximate solution is the solution of the ordinary Riemann problem with the left state being the reflected shock state. This gives $u^*(\infty) = 3129$ m/s.

The fair agreement of the numerical results with the approximate analytical solution of this problem suggests that the single wave approximation is quite accurate for the mass damped Riemann problem.

## 6. CONCLUSIONS

The mass-damped Riemann problem and its application to body acceleration was shown in this paper. From the examples, we see that the accuracy and stability of body motion calculations can be significantly improved over the conventional method when the body mass is small. The additional computational effort is very small compared to the flow calculations, because the mass-damped Riemann problem is solved only on the boundary points.

Our investigation on the mass-damped Riemann problem is preliminary and further study on both analytical and numerical solutions to the problem are needed. The application of this problem is not confined to improving force calculations. For example, we may ask if it is possible to use this problem to construct higher order Godunov-type methods for 1D Euler equations by replacing the body mass with some specially designed functions. A more extensive study on the error of the single wave approximation is also needed.

The example problems are solved using fixed grids. However, the procedure of force computation and conclusions on the improvement of force accuracy and stability should hold when moving grids are used.

## ACKNOWLEDGMENTS

The computation resources were provided in part by the University of Texas System Center for High Performance Computing and Pittsburgh Supercomputing Center. Financial support was provided by the Institute for Advanced Technology, under U.S. Army ARDEC Contract DAAA 21-93-C-0101.

## REFERENCES

1. R. Löhner, "Adaptive Remeshing for Transient Problems with Moving Bodies," in *11th Int. Conf. Num. Methods Fluid Dynamics*, edited by D. L. Dwoyer *et al.* (Springer-Verlag, Berlin, 1989), p. 379.
2. R. Courant and K. O. Friedrichs, *Supersonic Flow and Shock Waves* (Interscience, New York, 1948).
3. A. J. Chorin, *J. Comput. Phys.* **22,** 517 (1976).
4. D. Wilson, Z. Tan, and P. L. Varghese, *AIAA J.* **34,** 1341 (1996).
5. P. L. Roe, *Annu. Rev. Fluid Mech.* **18,** 337, (1985).
6. Z. Tan and P. L. Varghese, AIAA Paper 93-3320, 1993 (unpublished).
7. A. E. Seigel, "The Theory of High Speed Guns," AGARDograph 91, May 1965.
8. T. W. Roberts, *J. Comput. Phys.* **90,** 141 (1990).